

## Infrared phonon study of charge ordering in $\text{La}_{1/2}\text{Sr}_{3/2}\text{MnO}_4$

This article has been downloaded from IOPscience. Please scroll down to see the full text article.

2000 J. Phys.: Condens. Matter 12 9799

(<http://iopscience.iop.org/0953-8984/12/47/307>)

View [the table of contents for this issue](#), or go to the [journal homepage](#) for more

Download details:

IP Address: 171.66.16.221

The article was downloaded on 16/05/2010 at 07:01

Please note that [terms and conditions apply](#).

## Infrared phonon study of charge ordering in $\text{La}_{1/2}\text{Sr}_{3/2}\text{MnO}_4$

J H Jung<sup>†</sup>, H J Lee<sup>‡</sup>, T W Noh<sup>‡</sup> and Y Moritomo<sup>§</sup>

<sup>†</sup> Centre for Strongly Correlated Material Research, Seoul National University, Seoul 151-742, Korea

<sup>‡</sup> School of Physics and Research Centre for Oxide Electronics, Seoul National University, Seoul 151-742, Korea

<sup>§</sup> CIRSE, Nagoya University, Nagoya 464-8603 and PRESTO, JST, Japan

Received 9 October 2000

**Abstract.** We investigated the temperature- and polarization-dependent optic phonon modes of  $\text{La}_{1/2}\text{Sr}_{3/2}\text{MnO}_4$  using optical conductivity analyses. The phonon modes in the *ab*-plane are significantly changed, while those along the *c*-axis remain nearly constant with decreasing temperature. Below the charge-ordering temperature, the strength of the stretching phonon mode increases and its frequency becomes higher. These far-infrared phonon spectrum changes are closely related to the increase of the optical gap in the near-infrared region. Our experimental results suggest the importance of lattice distortion and strong electron–phonon interaction for the charge ordering in  $\text{La}_{1/2}\text{Sr}_{3/2}\text{MnO}_4$ .

### 1. Introduction

Doped manganites, with chemical formula  $\text{R}_{1-x}\text{A}_x\text{MnO}_3$  ( $\text{R} = \text{La, Nd, Pr}$ , and  $\text{A} = \text{Sr, Ca, Ba}$ ), have attracted great attention due to their unusual physical properties, such as colossal magnetoresistance [1]. Recently, many investigations have focused on charge-ordering phenomena, i.e., real-space ordering of the  $\text{Mn}^{3+}$  and the  $\text{Mn}^{4+}$  ions, which appear in samples with small bandwidths near  $x \sim 1/2$  [2, 3]. Quite interestingly, the charge orderings in manganites incorporate orbital orderings as well as antiferromagnetic spin orderings.

The layered perovskite  $\text{La}_{1/2}\text{Sr}_{3/2}\text{MnO}_4$  is another prototype material which shows charge ordering [4]. In this sample, charge ordering occurs below a charge-ordering temperature,  $T_{CO} \sim 220$  K [4], and a CE-type antiferromagnetic spin ordering occurs below a Néel temperature,  $T_N \sim 110$  K [5]. (It has no ferromagnetic metallic state for any temperature.) Below  $T_{CO}$ ,  $d_{3x^2-r^2}$  and  $d_{3y^2-r^2}$  orbital ordering also occurs [6]. For the  $\text{R}_{1-x}\text{A}_x\text{MnO}_3$  samples, it is difficult to investigate the charge and the lattice dynamics for a given direction due to the multi-domain nature of the samples. However, for  $\text{La}_{1/2}\text{Sr}_{3/2}\text{MnO}_4$ , such directional responses can be more easily investigated. Since  $\text{La}_{1/2}\text{Sr}_{3/2}\text{MnO}_4$  has  $\text{K}_2\text{NiF}_4$  crystal structure, the two-dimensional  $\text{MnO}_2$  layers, in which the charge ordering occurs, are structurally separated by insulating (La, Sr)O bilayers [7].

Optical measurements have been proven to be quite useful for investigating lattice dynamics and electronic structures in manganites [8–10]. Although there have been some reports on optical responses of charge-ordered manganites [11, 12], little work has been done on their optic phonon modes. In our earlier paper on optical properties of  $\text{La}_{1/2}\text{Sr}_{3/2}\text{MnO}_4$  [13], we concentrated on electronic structure changes including variation of an optical gap in the near-infrared and the visible region. To explain such structures, we performed a tight-binding

calculation and showed that the Jahn–Teller distortion of the  $\text{Mn}^{3+}$  ion in the  $ab$ -plane should be included. This work suggests that the lattice dynamics should be quite interesting.

In this paper, we report polarization-dependent optic phonon modes of  $\text{La}_{1/2}\text{Sr}_{3/2}\text{MnO}_4$ . While the phonon modes along the  $c$ -axis show little temperature dependence, those in the  $ab$ -plane show large changes below  $T_{CO}$ . In particular, the stretching phonon mode, which is known to be sensitive to the Mn–O distance, is strongly split and moves to higher frequencies, and its strength becomes increased. We also find that the temperature dependences of the stretching phonon mode strength and frequency show a clear correlation with that of the optical gap. These results support our earlier tight-binding calculation in indicating that the strong electron–phonon interaction (maybe of Jahn–Teller type) should be important for the charge ordering in  $\text{La}_{1/2}\text{Sr}_{3/2}\text{MnO}_4$ .

## 2. Experiments

Temperature- and polarization-dependent reflectivity spectra  $R(\omega)$  of a  $\text{La}_{1/2}\text{Sr}_{3/2}\text{MnO}_4$  single crystal were measured from 0.01 to 6.0 eV. (' $E \parallel ab$ ' and ' $E \parallel c$ ' indicate that the light polarization is pointing along the  $ab$ -plane and the  $c$ -axis, respectively.) To cover this wide photon energy region, a Fourier transform spectrophotometer was used for 0.01–0.5 eV and a grating monochromator was used for 0.4–6.0 eV. The temperature of the sample and the polarization of the incident light were varied using a liquid-He-cooled cryostat and grid-type polarizers, respectively. Using the Kramers–Kronig transformation, optical conductivity spectra  $\sigma(\omega)$  were obtained. Details of the reflectivity measurements and the Kramers–Kronig transformation [14] have been reported elsewhere.

## 3. Results and discussion

Figures 1(a) and 1(b) show the temperature-dependent  $R(\omega)$  for  $\text{La}_{1/2}\text{Sr}_{3/2}\text{MnO}_4$  for  $E \parallel ab$  and  $E \parallel c$ , respectively. The peaks below 0.1 eV originate from optic phonon modes and the broad peaks above 0.1 eV are due to interband transitions. For most of the measured photon energy regions, especially below 0.1 eV, the  $R(\omega)$  show strong anisotropies between  $E \parallel ab$  and  $E \parallel c$ . With decreasing temperature, the  $R(\omega)$  show large changes for  $E \parallel ab$ , but small changes for  $E \parallel c$ .

In the inset of figure 2, we show the polarization-dependent optic phonon modes of  $\text{La}_{1/2}\text{Sr}_{3/2}\text{MnO}_4$  at 290 K. The solid and dotted lines represent  $\sigma(\omega)$  for  $E \parallel ab$  and  $E \parallel c$ , respectively. Apparently, there are four optic phonon modes located around 173 (222), 286 (374), 367 (419), and 600 (476)  $\text{cm}^{-1}$  for  $E \parallel ab$  ( $E \parallel c$ ). From group theory, seven infrared-active phonon modes are expected to be observed in the  $\text{K}_2\text{NiF}_4$  structure with tetragonal  $I4/mmm$  symmetry, as represented by  $\Gamma_{opt} = 3A_{2u} + 4E_u + 2A_{1g} + 2E_g + B_{2u}$  [15]. In the  $ab$ -plane, the phonon modes corresponding to  $4E_u$  can be observed. From the lowest-frequency modes, they may correspond to one external mode, two bending modes, and one stretching mode. Along the  $c$ -axis, three phonon modes corresponding to  $3A_{2u}$  should be observed. However, four phonon modes can be clearly observed along this direction. The existence of one more phonon mode suggests that an additional phonon mode might originate from local lattice distortions.

The temperature-dependent  $\sigma(\omega)$  for  $E \parallel ab$  are shown in figure 2. (The temperature-dependent changes of  $\sigma(\omega)$  for  $E \parallel c$  are quite small.) With decreasing temperature, the bending and stretching phonon modes become changed near  $T_{CO} \sim 220$  K. At 15 K, at least seven phonon modes can be observed. In addition, frequencies of the bending and stretching

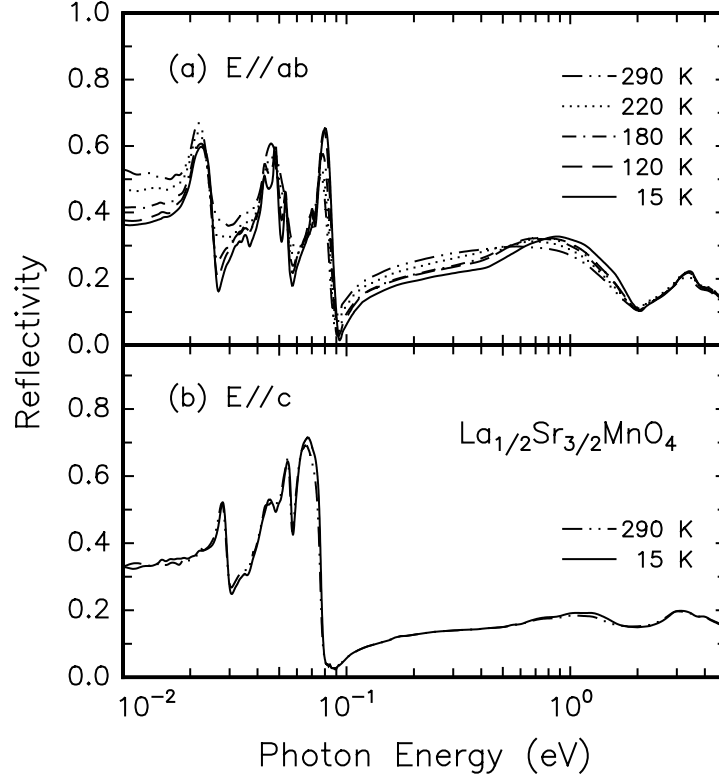


**Figure 1.** Reflectivity spectra of  $\text{La}_{1/2}\text{Sr}_{3/2}\text{MnO}_4$  for (a)  $E \parallel ab$  and (b)  $E \parallel c$ .

modes are significantly modified below  $T_{CO}$ . Similar phonon mode changes below  $T_{CO}$  are observed in other charge-ordered transition metal oxides, such as  $\text{La}_{1/3}\text{Sr}_{2/3}\text{FeO}_3$  [16] and  $\text{La}_{5/3}\text{Sr}_{1/3}\text{NiO}_4$  [17]. These phonon mode changes have been interpreted in terms of either phonon splittings or the appearance of new phonon modes [16, 17]. A charge ordering will give rise to lower crystal symmetry, and leads to lifting of the degeneracy of phonon modes. As a result, splitting of the phonon modes will occur. Another possibility is that charge ordering will give rise to the formation of a superlattice, which leads to folding of the phonon dispersion branch. Then, new phonon modes will appear.

To obtain more quantitative information, we fit the optic phonon modes in figure 2 with a series of Lorentz oscillators:

$$\sigma(\omega) = \sum_i \frac{S_i \Gamma_i \omega^2}{(\omega^2 - \omega_i^2)^2 + \Gamma_i^2 \omega^2} \quad (1)$$

where  $S_i$ ,  $\omega_i$ , and  $\Gamma_i$  represent the strength, the frequency, and the damping constant of the  $i$ th Lorentz oscillator, respectively. The fitting results at 290 and 15 K for  $E \parallel ab$  are summarized in table 1, and those for  $E \parallel c$  are summarized in table 2.

Two research groups have already reported phonon mode studies of  $\text{La}_{1/2}\text{Sr}_{3/2}\text{MnO}_4$ . First, Calvani *et al* [18] investigated optical responses of fine  $\text{La}_{1/2}\text{Sr}_{3/2}\text{MnO}_4$  powders which were diluted in CsI. Although they observed temperature-dependent phonon changes similar to ours, they could not separate the phonon responses for  $E \parallel ab$  and  $E \parallel c$ . Moreover, their reported values of phonon frequencies were quite different from ours. In powder geometry, a

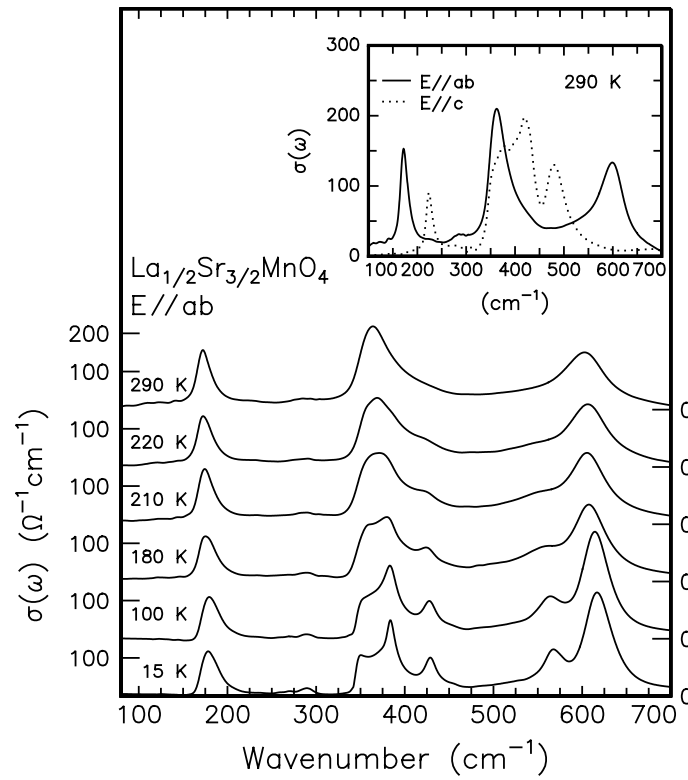


**Figure 2.** Temperature-dependent optic phonon modes for  $E \parallel ab$ . In the inset, the solid and dotted lines represent the phonon modes at 290 K for  $E \parallel ab$  and  $E \parallel c$ , respectively.

**Table 1.** Phonon fitting parameters at 290 and 15 K for  $E \parallel ab$ .

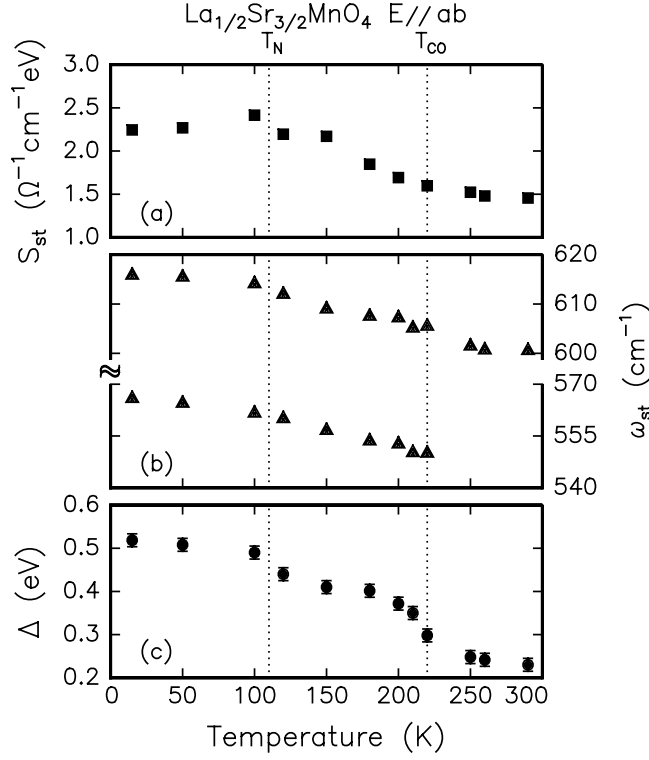
$S_i$ ( $\Omega^{-1} \text{ cm}^{-1} \text{ eV}$ )		$\omega_i$ ( $\text{cm}^{-1}$ )		$\Gamma_i$ ( $\text{cm}^{-1}$ )	
290 K	15 K	290 K	15 K	290 K	15 K
0.61	0.43	$173 \pm 2$	$180 \pm 3$	$22 \pm 5$	$19 \pm 1$
0.13	0.13	$286 \pm 1$	$286 \pm 3$	$46 \pm 5$	$46 \pm 1$
	0.30		$354 \pm 3$		$17 \pm 2$
1.89	0.68	$367 \pm 4$	$384 \pm 1$	$53 \pm 5$	$21 \pm 1$
	0.36		$426 \pm 3$		$27 \pm 1$
	0.55		$565 \pm 2$		$37 \pm 6$
1.47	1.65	$600 \pm 2$	$618 \pm 1$	$77 \pm 10$	$36 \pm 1$

strong resonant absorption will occur at a frequency where the dielectric constant of the bulk is close to  $-2\epsilon_h$ , which is the dielectric constant of the surrounding medium (i.e. CsI) [19]. Therefore, the phonon frequencies obtained from the powder samples should be located at higher frequencies than the actual phonon frequencies. Second, Ishikawa *et al* [20] reported reflectivity spectra of the single crystal *only* for  $E \parallel ab$ . Although their reflectivity results were similar to ours for  $E \parallel ab$ , they did not report details of the phonon parameters.

Figure 3(a) shows the temperature-dependent strength  $S_{st}$  of the stretching phonon mode for  $E \parallel ab$ . Note that the stretching phonon mode is sensitive to the Mn–O distance. At low

**Table 2.** Phonon fitting parameters at 290 and 15 K for  $E \parallel c$ .

$S_i$ ( $\Omega^{-1} \text{ cm}^{-1} \text{ eV}$ )		$\omega_i$ ( $\text{cm}^{-1}$ )		$\Gamma_i$ ( $\text{cm}^{-1}$ )	
290 K	15 K	290 K	15 K	290 K	15 K
0.27	0.28	$222 \pm 1$	$226 \pm 2$	$17 \pm 1$	$17 \pm 3$
1.33	1.31	$374 \pm 3$	$374 \pm 3$	$50 \pm 4$	$50 \pm 3$
0.93	1.15	$419 \pm 1$	$423 \pm 3$	$33 \pm 3$	$33 \pm 5$
0.99	1.00	$476 \pm 3$	$483 \pm 3$	$55 \pm 1$	$43 \pm 5$

**Figure 3.** Temperature dependences of the stretching mode (a) strength ( $S_{st}$ ) and (b) frequency ( $\omega_{st}$ ). In (c), the optical gap ( $\Delta$ ), obtained from figure 4, is shown.

temperatures, there are two phonon modes located around 565 and 618  $\text{cm}^{-1}$ ; the strengths of these two modes are summed to obtain values of  $S_{st}$ . With decreasing temperature,  $S_{st}$  starts to increase below  $T_{CO}$  and nearly saturates below  $T_N$ . Generally, the strength of the Lorentz oscillator is known to be proportional to the amplitude of lattice distortions [21]. In figure 3(b), we show the temperature-dependent frequency  $\omega_{st}$  of the stretching phonon mode. With decreasing temperature,  $\omega_{st}$  significantly increases below  $T_{CO}$  and nearly saturates below  $T_N$ . The frequency of the low-lying mode below  $T_{CO}$ , located around 550  $\text{cm}^{-1}$ , also moves to higher values.

Phonon frequency shifts have been observed near phase transitions in numerous manganites. For example,  $\text{La}_{0.7}\text{Ca}_{0.3}\text{MnO}_3$  experiences a transition from a paramagnetic insulator to a ferromagnetic metal near the Curie temperature  $T_C$ . Kim *et al* [22] reported

stretching phonon mode hardening below  $T_C$ . In  $\text{La}_{0.7}\text{Ca}_{0.3}\text{MnO}_3$ , the stretching phonon shift was explained by the electron–phonon coupling and the electronic screening originating from the double-exchange model [23]. However, in  $\text{La}_{1/2}\text{Sr}_{3/2}\text{MnO}_4$ , the double-exchange interaction is negligible due to the lack of ferromagnetism and/or metallicity, but charge ordering occurs. Therefore, to explain the phonon shift in  $\text{La}_{1/2}\text{Sr}_{3/2}\text{MnO}_4$ , we should consider the strong electron–phonon interaction and/or some interactions to localize the electrons, such as intersite Coulomb repulsion. In fact, Lee and Min [24] calculated the lattice dynamics near  $T_{CO}$  on the basis of a Hamiltonian incorporating a small polaron with strong nearest-neighbour repulsion. They obtained results for strong renormalization of the phonon frequency near  $T_{CO}$  similar to those depicted in figure 3(b).

Figures 4(a) and 4(b) show the temperature-dependent  $\sigma(\omega)$  for  $\text{La}_{1/2}\text{Sr}_{3/2}\text{MnO}_4$  in the higher-frequency region for  $E \parallel ab$  and  $E \parallel c$ , respectively. At a glance, we can see large anisotropies in  $\sigma(\omega)$ . Values of the optical gap  $\Delta$  are obtained from the point at which the abscissa is crossed with a linear extrapolation of  $\sigma(\omega)$ , and shown in figure 3(c). With decreasing temperature, the values of  $\Delta$  are sharply increased and spectral weights below 0.8 eV are transferred to higher frequency for  $E \parallel ab$ , while those for  $E \parallel c$  are nearly temperature independent. For such a strong temperature dependence in the  $ab$ -plane, we showed that  $\sigma(\omega)$  could be explained by the enhancement of the charge ordering stabilized by the Jahn–Teller distortion [13].

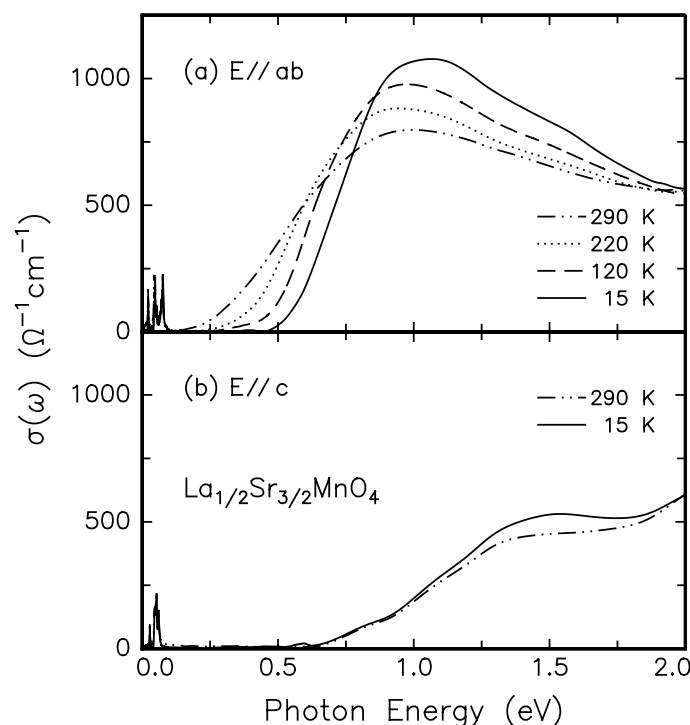


**Figure 4.**  $\sigma(\omega)$  in the near-infrared and visible region for (a)  $E \parallel ab$  and (b)  $E \parallel c$ .

In order to understand the close relationship between the lattice (Jahn–Teller distortion) and charge dynamics, we summarize the temperature dependences of  $S_{st}$ ,  $\omega_{st}$ , and  $\Delta$  for  $E \parallel ab$  in figure 3. Note that the temperature dependences of  $S_{st}$ ,  $\omega_{st}$ , and  $\Delta$  are quite similar. All three quantities are nearly constant above  $T_{CO}$ , increase for  $T_N < T < T_{CO}$ , and become saturated

for  $T < T_N$ . These strong correlations between the stretching phonon mode and the optical gap can be explained by assuming that the charge ordering is accompanied by the strong electron–phonon interaction due to the Jahn–Teller-type distortion of the  $\text{Mn}^{3+}$  ion. Below  $T_{CO}$ , charge ordering occurs, so the optical gap should increase as shown in figure 3(c). In addition, there should exist ordering of the  $\text{Mn}^{3+}\text{O}_6$  and the  $\text{Mn}^{4+}\text{O}_6$  octahedra, and the static Jahn–Teller distortion should occur at the  $\text{Mn}^{3+}\text{O}_6$  octahedra. Then, the lattice distortion corresponding to the Jahn–Teller distortion should increase, consistently with figure 3(a). Finally, due to the charge ordering and the strong electron–phonon interaction, the phonon frequency of the Jahn–Teller mode should increase consistently with figure 3(b). These results suggest the importance of the Jahn–Teller distortion for charge ordering in manganites, which is in good agreement with other experimental [25] and theoretical [26] results.

#### 4. Summary

In summary, we have investigated the optic phonon modes of  $\text{La}_{1/2}\text{Sr}_{3/2}\text{MnO}_4$  with temperature-dependent and polarization-dependent optical studies. Below the charge-ordering temperature, the stretching phonon mode is significantly changed with a strong correlation with the optical gap. This result may suggest importance of the Jahn–Teller distortion for charge-ordering phenomena in  $\text{La}_{1/2}\text{Sr}_{3/2}\text{MnO}_4$ .

#### Acknowledgments

We acknowledge Professor Jaejun Yu and Se-Jung Oh for helpful discussions. This work was supported by Ministry of Science and Technology through the Creative Research Initiative Programme. JHJ and HJL were also supported by the Ministry of Education through the BK-21 Programme. The work by YM was supported by a Grant-In-Aid for Scientific Research from the Ministry of Education, Science, Sports, and Culture.

#### References

- [1] Jin S, Tiefel T H, McCormack M, Fastnacht R A, Ramesh R and Chen L H 1994 *Science* **264** 413
- [2] Chen C H and Cheong S-W 1996 *Phys. Rev. Lett.* **76** 4042
- [3] Mori S, Chen C H and Cheong S-W 1998 *Nature* **392** 473
- [4] Moritomo Y, Tomioka Y, Asamitsu A, Tokura Y and Matsui Y 1995 *Phys. Rev. B* **51** 3297
- [5] Sternlieb B J, Hill J P, Wildgruber U C, Luke G M, Nachumi B, Moritomo Y and Tokura Y 1996 *Phys. Rev. Lett.* **76** 2169
- [6] Murakami Y, Kawada H, Kawata H, Tanaka M, Arima T, Moritomo Y and Tokura Y 1998 *Phys. Rev. Lett.* **80** 1932
- [7] Moritomo Y, Asamitsu A, Kuwahara H and Tokura Y 1996 *Nature* **380** 141
- [8] Okimoto Y, Katsufuji T, Ishikawa T, Urushibara A, Arima T and Tokura Y 1995 *Phys. Rev. Lett.* **75** 109
- [9] Kim K H, Jung J H and Noh T W 1998 *Phys. Rev. Lett.* **81** 1517
- [10] Quijada M, Černe J, Simpson J R, Drew H D, Ahn K H, Millis A J, Shreekala R, Ramesh R, Rajeswari M and Venkatesan T 1998 *Phys. Rev. B* **58** 16 093
- [11] Calvani P, De Marzi G, Dore P, Lupi S, Maselli P, D'Amore F, Gagliardi S and Cheong S-W 1998 *Phys. Rev. Lett.* **81** 4504
- [12] Liu H L, Cooper S L and Cheong S-W 1998 *Phys. Rev. Lett.* **81** 4684
- [13] Jung J H, Ahn J S, Yu J, Noh T W, Lee J, Moritomo Y, Solovyev I and Terakura K 2000 *Phys. Rev. B* **61** 6902
- [14] Jung J H, Kim K H, Eom D J, Noh T W, Choi E J, Yu J, Kwon Y S and Chung Y 1997 *Phys. Rev. B* **55** 15 489
- [15] Tajima S, Ido T, Ishibashi S, Itoh T, Eisaki H, Mizuo Y, Arima T, Takagi H and Uchida S 1991 *Phys. Rev. B* **43** 10 496
- [16] Ishikawa T, Park S K, Katsufuji T, Arima T and Tokura Y 1998 *Phys. Rev. B* **58** R13 326
- [17] Katsufuji T, Tanabe T, Ishikawa T, Fukuda Y, Arima T and Tokura Y 1996 *Phys. Rev. B* **54** R14 230



- [18] Calvani P, Paolone A, Dore P, Lupi S, Maselli P, Medaglia P G and Cheong S-W 1996 *Phys. Rev. B* **54** R9592
- [19] Noh T W, Kaplan S G and Sievers A J 1990 *Phys. Rev. B* **41** 307
- [20] Ishikawa T, Ookura K and Tokura Y 1999 *Phys. Rev. B* **59** 8367
- [21] Gervais F 1982 *Infrared and Millimeter Waves* (New York: Academic)
- [22] Kim K H, Gu J Y, Choi H S, Park G W and Noh T W 1996 *Phys. Rev. Lett.* **77** 1877
- [23] Zener C 1951 *Phys. Rev.* **82** 403  
Anderson P W and Hasegawa H 1955 *Phys. Rev.* **100** 675
- [24] Lee J D and Min B I 1997 *Phys. Rev. B* **55** R14 713
- [25] Moritomo Y, Nakamura A, Mori S, Yamamoto N, Ohoyama K and Ohashi M 1997 *Phys. Rev. B* **56** 14 879
- [26] Mizokawa T and Fujimori A 1997 *Phys. Rev. B* **56** R493